UNIVERSITY OF VERONA

DEPARTMENT OF

Diagnostic and Public Health

GRADUATE SCHOOL OF

Health and Life Sciences

DOCTORAL PROGRAM IN

Inflammation, Immunity and Cancer

XXXI / 2015

TITLE OF THE DOCTORAL THESIS

GENETIC, EPIGENETIC AND MICRO-ENVIRONMENTAL MARKERS AS PREDICTORS OF PROGNOSIS, RESPONSE AND RESISTANCE TO CHEMOTHERAPY, TARGETED AGENTS AND IMMUNOTHERAPY IN RESECTED SQUAMOUS CELL LUNG CARCINOMA (SQLC).

S.S.D. MED/06

Coordinatore: Prof.ssa Gabriela Constantin

Firma _____

Tutor: Prof. Emilio Bria

Firma _____

Dottorando: Dott.ssa Sara Pilotto

Firma _____

TABLE OF CONTENTS

SUMMARY

Diversamente dall'adenocarcinoma polmonare, per il carcinoma polmonare a cellule squamose (SQLC) non sono ancora disponibili terapie a bersaglio molecolare, sebbene una serie di vie di segnale sia risultata costantemente alterata. A questo proposito, è necessario chiarire l'eventuale impatto prognostico e/o predittivo dei potenziali *drivers*, al fine di studiare il background molecolare dei pazienti con SQLC. Una delle principali strategie di ricerca emergenti in ambito oncologico si basa sullo studio del genoma di pazienti con risposta anomala al trattamento o con prognosi inattesa. Adottando questa idea, abbiamo analizzato retrospettivamente una serie multicentrica di 573 pazienti affetti da SQLC sottoposti a resezione chirurgica e abbiamo costruito uno dei primi modelli di classificazione del rischio per SQLC, successivamente convalidato in una coorte più ampia di oltre 1000 pazienti. Questo modello, basato su una combinazione di parametri semplici clinico-patologici, è stato in grado di stratificare in modo efficace i pazienti con SQLC con una buona accuratezza prognostica. Una volta identificati i *'migliori'* e *'peggiori'* dal punto di vista prognostico, abbiamo studiato il loro ritratto molecolare, principalmente mediante sequenziamento (NGS), e il loro profilo di espressione per identificare alterazioni molecolari ricorrenti ed esplorare la loro associazione prognostica. Sessanta e quarantasette pazienti sono stati rispettivamente valutati come coorte di training e validazione. La variazione del numero di copie (CNV) era l'evento genomico più frequente. Le alterazioni molecolari erano distribuite indipendentemente dalla prognosi, ad eccezione delle mutazioni di *DDR2* nel gruppo con buona prognosi e la perdita di *SMAD4* nel gruppo con prognosi sfavorevole. L'asse PI3KCA/mTOR rappresentava la via di segnale più frequentemente alterata (42%) e le mutazioni di *PI3KCA* e l'alto CNV di *RICTOR* sono stati identificati solo nel sottogruppo a prognosi sfavorevole. All'analisi del trascrittoma, i pazienti con alto CNV di *RICTOR* avevano una maggiore attivazione della via di segnale PI3KCA/mTOR. Lo scopo ultimo del progetto era di valutare il profilo molecolare degli SQLC resecabili utilizzando tecnologie moderne al fine di identificare quelle aberrazioni molecolari potenzialmente in grado di prevedere la probabilità di recidiva e l'efficacia di agenti a bersaglio molecolare. Questa analisi integrata e multi-step eseguita in quasi un

centinaio di pazienti SQLC resecati ha identificato vie di segnale alterate con un impatto biologico rilevante sull'oncogenesi di SQLC, rivelando l'elevato CNV di *RICTOR* come bersaglio terapeutico candidato all'inibizione selettiva in SQLC.

ABSTRACT

Differently from lung adenocarcinoma, effective targeted therapies for lung squamous-cell cancer (SQLC) are still missing, although a series of molecular pathways are constantly altered. In this regard, the prognostic and/or predictive impact of potential *drivers* needs to be elucidated, in order to create a global portrait of SQLC patients. Nowadays, one of the main emerging research strategies in cancer is centered on the study of the genome of exceptional responder and prognostic outlier patients. Adopting this idea, we retrospectively analysed a multicenter series of 573 surgically resected SQLC patients and we built one of the first risk classification model for SQLC, which was afterwards validated in a larger cohort of more than 1000 patients. This model, based on a combination of simple and easily available clinicopathological parameters, was able to effectively stratify resected SQLC patients in risk classes with a good prognostic accuracy. Once identified the best and worst prognostic performers, we investigated their molecular portrait, principally by next-generation sequencing (NGS), and their expression profile to identify recurrent molecular alterations and explore their association with prognosis. Sixty and forty-seven patients were evaluated as training and validation cohort, respectively. Copy number variation (CNV) was the most frequent genomic event. Molecular alterations were distributed regardless of prognosis, except from *DDR2* mutations in good prognosis group and *SMAD4* loss in poor prognosis group. The potentially druggable PI3KCA/mTOR axis represented the most frequently altered pathway (42%), with *PI3KCA* mutations and *RICTOR* high gain reported only in poor prognosis group. Upon transcriptome analysis, *RICTOR* high gain patients presented an increased pathway activity. The final aim of the overall project was to evaluate the molecular profile of outliers resected SQLC taking the advantage to adopt modern technologies in order to identify those molecular aberrations potentially able to predict the probability of disease recurrence and the efficacy of agents selectively targeting these candidate pathways. This integrated multi-step analysis performed in almost one hundred resected SQLC patients identified altered pathways with a biological impact in SQLC oncogenesis, revealing *RICTOR* high gain as a candidate therapeutical target for selective inhibition in SQLC.

INTRODUCTION

In recent years, the identification of targetable oncogenic drivers, together with the introduction in clinical practice of a therapeutic decision-making process including tumor genotyping, provided the proof-of-principle that non-small-cell lung cancer (NSCLC) is composed by a group of heterogeneous diseases, which require a personalized approach [1]. Particularly in the context of adenocarcinoma, reliable evidence are available suggesting that cancer development and progression may be addicted through aberrant pathways specifically triggered by genetic abnormalities, constitutively acting as oncogenic drivers. Emblematic examples of such dependency are represented by *EGFR* mutant [2-4] and *ALK* rearranged adenocarcinoma [5, 6], where the treatment with their specific tyrosine kinase inhibitors significantly change the disease natural history.

Nevertheless, epidemiologically relevant subtypes of NSCLC, as squamous-cell lung cancer (SQLC, approximately 25-30% of NSCLC), still lack of a reliable clinico-pathological and molecular characterization, in order to both stratify patients according to their prognosis and predict their potential susceptibility to targeted therapy. Regarding candidate clinico-pathological factors, the TNM stage represents the most reliable prognostic predictor in NSCLC patients [7]. In addition to TNM staging, the prognostic significance of the predominant histologic patterns has been validated in lung adenocarcinoma, whereas a similar prognostic role has been observed for histological subtyping of SQLC (i.e. keratinizing, non-keratinizing, basaloid and clear cell subtypes) [8, 9]. However, in this uncertain landscape, several investigated pathological factors (including single cell invasion, tumor budding, nuclear diameter, number of metastatic lymph nodes, lymphatic/vascular and pleural invasion) demonstrated a potential prognostic role in different series of resected SQLC, retrospectively analyzed [8-10].

With regard to molecular abnormalities, the Cancer Genome Atlas Research Project published the largest genomic characterization of SQLC, providing a comprehensive landscape of genomic and epigenomic alterations featuring the early stage of the disease. This study validated the existence of potentially druggable genes or pathways and provided the first evidence of the mutual exclusivity of genomic alterations, some of which potentially targetable by investigational agents

[10]. Nevertheless, only few clinical trials are ongoing to advance the development of targeted therapies in SQLC [11]. Recently, the therapeutic opportunities for lung cancer patients have further expanded with the introduction of immunotherapy, particularly in those tumors that feature a strong genetic diversity, such as SQLC [12]. Although the overexpression of programmed death-ligand 1 (PD-L1) seems to increase the chance to respond to immune checkpoint inhibitors in the advanced disease setting, its prognostic role is still debatable [13].

In this rapidly evolving landscape, the identification of the appropriate risk category for each patient represents a promising strategy for two main reasons [14]. First, in the context of an early stage disease, the prognostic stratification might allow selection of those patients with a more favorable risk-benefit ratio from adjuvant treatments. Second, from an exploratory point-of-view, the molecular characterization of patients featured by a different prognosis, by applying the modern technologies, could help in the identification of those genomic and epigenomic aberrations potentially able to predict the probability of disease recurrence (prognostic factors) and the efficacy of agents selectively targeting these candidate pathways (predictive factors). Applying this research strategy in the field of lung cancer, we aim to create a prognostic nomogram for resected SQLC based on clinicopathological and molecular biomarkers, which may directly determine patient predictions, risk stratification and treatment assignment with targeted agents, according to the emerged findings in the preclinical setting. This strategy, may thus successfully integrate the known clinical with the newest genetic acquisitions into prognostic (and hopefully) predictive nomograms.

MATERIAL AND METHODS

The overall project included three main steps:

1. Building of a clinical risk classification model for resected SQLC.
2. Validation of this clinical classification model in the context of an external cohort of resected SQLC.
3. Analysis of the molecular portrait of prognostic outlier patients in order to identify differentially expressed and potentially druggable molecular targets.

Building of a clinical risk classification model for resected SQLC.

A step-by-step protocol was followed according to the methodological approach for building a nomogram for cancer prognosis proposed by *Iasonos et al.* [15], with respect to the Reporting Recommendations for Tumor Marker Prognostic Studies (REMARK) criteria for the conduction of a retrospective study in the context of an unselected population [16, 17].

Patients' population.

Resected SQLC cases with stored tissue available for biomolecular analyses and at least 2 years follow-up, who underwent surgery since 2009 in five Italian institutions (University of Verona; Regina Elena National Cancer Institute, Rome; University of Torino; University of Perugia; University-Foundation of Chieti), were considered eligible. A merged database of data was accomplished. Pathological diagnosis was made according to the World Health Organization (WHO) classification and the American Joint Committee on Cancer (AJCC); the Union for International Cancer Control (UICC) TNM system (7th edition) for lung cancer was applied for disease staging.

Endpoints.

The aim of this first part of the analysis was to develop and validate a clinico-pathological prognostic risk-class model to identify the best and worst performers in the context of a multicenter population of resected SQLC. The model was developed on the basis of a multivariate analysis exploring the independent impact of clinico-pathological factors on Overall Survival (OS: time between diagnosis and death for any cause), Cancer Specific Survival (CSS: time between diagnosis and death due to cancer progression) and Disease Free Survival (DFS: time between

diagnosis and local/distant recurrence, onset of secondary cancer or death for any cause).

Statistical analysis.

Descriptive statistics was used to summarize pertinent study information. Follow-up was analyzed and reported according to *Shuster et al.* [18]. Associations between variables were analysed according to the Pearson Chi-Square test. The Hazard Ratio (HR) and the 95% confidence intervals (95% CI) was estimated using the Cox univariate model [19]. A multivariate proportional hazard model was developed using stepwise regression (forward selection, enter limit and remove limit p=0.10 and p=0.15, respectively), in order to identify independent predictors of outcomes. The assessment of interactions between significant investigational variables was taken into account when developing the multivariate model. In presence of non-linear distribution of ratios of continuous variables, the receiver operating characteristic (ROC) curve analysis was adopted for dichotomization according to outcome [20, 21]. The ROC curve analysis allowed to estimate the area under the curve (AUC) with standard error (SE) and 95% confidence interval, in order to provide a list of sensitivity, specificity, likelihood ratios, and positive and negative predictive values for all possible threshold values, and to calculate the difference between the areas under the ROC curves, with standard error, 95% confidence interval and P-value [22]. OS, CSS and DFS were calculated by the Kaplan-Meier product limit method from the date of the surgery until relapse, death due to cancer and/or death for any cause. Curves were reported for those prognostic factors which resulted independent at the multivariate analysis. The log-rank test was used to assess differences between subgroups. Significance was defined at the $p<0.05$ level. The SPSS®(18.0), R® (2.6.1), and MedCalc® (14.2.1) licenced statistical programs were used for all analyses.

Prognostic score assessment.

The log-HR obtained from the Cox model was used to derive weighting factors of a continuous prognostic index, aimed to identify differential outcomes' risks. Coefficients estimates were 'normalized' dividing by the smallest one and rounding the resulting ratios to the nearest integer value [23]. Thus, a continuous score assigning to patients an 'individualized' risk was generated. Two different methods

were adopted to derive risk classes [24]:

(i) for Model A, the score was dichotomized according to prognosis with the ROC analysis (the best 'splitter' cutoff is determined) [21];

(ii) for Model B, patients' outcomes (OS, CSS and DFS) were displayed by dividing patients into three risk classes, by considering cutoffs chosen at approximately equal distance along the range of values [23].

Internal validation analysis.

In order to address the multivariate model overfit and to validate the results, a cross-validation technique, which evaluates the replication stability of the final Cox multivariate model in predicting all outcomes was also investigated, using a re-sampling procedure [15, 25, 26]. This technique generates a number of simulation datasets (at least 100, each approximately 80% of the original size), by randomly selecting patients from the original sample, in order to establish the consistency of the model across less-powered patient' samples. Risk classes was generated based on the combination of the found risk factors. The ROC analysis allowed to assess the predictive accuracy of the prognostic model, by the area under the curve (AUC) determination [22].

The Harrell's guidelines for the identification of the correct number of covariates were taken into account for the power analysis (the number of deaths should have be more than 10 times greater than the number of investigated predictors, so that the expected error from the Cox model would be less than 10%) [27].

Validation of this clinical classification model in the context of an external cohort of resected SQLC.

Patients' population.

Patients with resected SQLC who had stored tissue available for pathological analysis and at least 2 years of follow-up after removal of the primary tumor and who had undergone surgery from January 2002 to December 2012 in six Italian institutions were considered eligible. A merged database was created. The pathological diagnosis was made according to the WHO classification and the American Joint Committee on Cancer [28]. To be consistent with the previously published prognostic model, the Union for International Cancer Control TNM

staging system (seventh edition) for lung cancer was applied for disease staging [29].

Endpoints.

The main aim of the second part of the project was to validate the already-published clinical risk classification model in a larger multicenter series of patients. Moreover, we aimed to analyse the impact of adjuvant and neoadjuvant treatment (ANT) in patients with resected SQLC both in the overall cohort and in the different risk classes stratified according to the prognostic model.

Statistical analysis.

Descriptive statistics were used to summarize pertinent study information. The reverse method was applied to calculate the median follow-up [30]. Associations between variables were analyzed according to the Pearson chi-square test for categorical variables and the t-test for continuous variables. The HR and the 95% CIs were estimated by using the Cox univariate model. Each patient was assigned a score to classify individual risk of disease recurrence on the basis of those clinicopathological factors included in the published prognostic model: age (≤68 *versus* >68 years), T descriptor according to seventh edition of the TNM classification (1 or 2 *versus* 3 or 4), lymph node status (negative *versus* positive) and grading (1 or 2 *versus* 3). Kaplan-Meier analysis for DFS, CSS, and OS was performed according to the three-class risk model B (with low risk equal to a score of 0–2, intermediate risk equal to a score of 3–4, and high risk equal to a score of 5–6).8 The log-rank test was adopted to compare the survival curves. The Harrell's C-statistic was adopted to measure the predictive accuracy of the risk model [27]. The effect of ANT was adjusted with the propensity score (PS) by applying the method of nearest neighbor matching within a specified caliper distance. In this regard, the PS match creates groups of patients with a similar probability of receiving the treatment on the basis of their baseline characteristics to minimize the differences in patients' covariates, which could become confounding factors in the examination of treatment effects in a nonrandomized cohort [31]. Specifically, a PS for the likelihood of receiving ANT was calculated by using a covariate adjustment method including a series of clinicopathological factors that might influence doctors' choice about treatment: age, T descriptor according to seventh edition of

the TNM classification, lymph node status, and grading. According to these covariates, an unmatched sample of patients was identified. By using a 1:1 nearest neighbor matching algorithm that pairs patients with the closest PS within a defined limit (calipers of width equal to 0.2), the PS yielded two well-matched patient cohorts (logistic regression estimation algorithm). Significance was defined at the $p<0.05$ level. The SPSS®(18.0), R® (2.6.1), and MedCalc® (14.2.1) licenced statistical programs were used for all analyses.

Analysis of the molecular portrait of prognostic outlier patients.

Patients.

Resected SQLC patients with available formalin-fixed paraffin embedded (FFPE) blocks for molecular analysis with at least 2 years of follow-up after removal of the primary tumor, who underwent surgery since 2009 in three Italian institutions (University of Verona, Regina Elena National Cancer Institute - Rome, University of Turin provided data for the training set) and classified as good prognosis (GP) or poor prognosis (PP) in terms of DFS according to the previously built and validated three-class prognostic model, were considered eligible. University of Perugia provided an additional cohort of resected SQLC samples to be available as a validation set.

Somatic mutations (SM) and copy number variations (CNV) analysis by next-generation sequencing (NGS) on tumor samples.

DNA was obtained from matched tumor and non-neoplastic lung included in formalin-fixed paraffin embedded (FFPE) blocks. In particular, tumor DNA from FFPE was prepared after enrichment for neoplastic cellularity to at least 70% using manual microdissection of 10 consecutive 4-μm FFPE sections. Sections were then purified using the QIAamp DNA FFPE Tissue Kit (Qiagen) and qualified. A Tissue Macro Array (TMA) was built including all cases (three cores each ones) and three normal lung as control. Matched tumor/normal DNA from all FFPE samples was subjected to targeted NGS. The Comprehensive Cancer panel (CCP) was used to investigate the mutational status of 409 genes in training set (details on target regions of the commercial panel are at http://www.thermofisher.com). Tumor Mutational Burden (TMB) was estimated according to *Rizvi et al*. [32]. Briefly, number of somatic mutations identified in each sample is divided by the number of

base pair covered by CCP for a genomic space of 1.7Mb. Regarding the mutational analysis of validation set, a custom panel targeting 56 genes was selected upon the results from the discovery screen using CCP, and published exome and targeted sequencing studies [10, 33, 34]: *AKT1, ALK, APC, ARID1A, ARID2, ATM, BAP1, BCL2L1, CCND1, CCND2, CDH1, CDH10, CDKN2A, CHD7, CUL3, DDR2, EGFR, ERBB2, FBXW7, FGFR1, FGFR2, FGFR3, FLT3, FRS2, KAT6A, KDM6A, KEAP1, KMT2D, KRAS, MDM2, MET, MYC, MYCL, NF1, NFE2L2, NOTCH1, NOTCH2, NOTCH3, NRAS, PAPPA2, PIK3CA, PTEN, RASA1, RB1, RICTOR, SMAD4, SMARCA4, SOX2, STAT3, TERT, TET2, TIE1, TP53, TP63, TSC1* and *TSC2*. Regarding CNV analysis of cell lines, a custom panel targets selected regions of 36 genes selected upon the results of published whole genome sequencing and exome data [33, 34]: *AKT1, APC, BCL2L1, CCND1, CCND2, CDKN2A, CDKN2B, DDR2, EGFR, ERBB2, FGFR1, FGFR2, FGFR3, FRS2, KIT, MDM2, MET, MYC, MYCL, MYCN, NFE2L2, NOTCH1, PDGFRA, PIK3CA, PTEN, RB1, RICTOR, SMAD4, SOX2, TERT, TET2, TIAF1, TP53, TP63, TSC2* and *TUBG1*. An orthogonal validation using FISH or qPCR was performed to confirm a subset of the CNVs identified. In this case, only concordant results between methodical were reported. In term of cut-off, CNV > 5 was defined as high gain, while CNV ≤ 5 as low gain.

CNV validation by Quantitative PCR (q-PCR).

RNA was obtained from 10 consecutive 6-µm FFPE sections using RecoverAll total nucleic acid isolation kit protocol (ThermoFisher). RNA was quantified using Qubit RNA BR Assay Kit (ThermoFisher) and qualified using Agilent RNA 6000 Nano Kit (Agilent Technologies). A RNA Integrity Number (RIN) over 5 was considered suitable for transcriptomic analysis. Quantitative PCR analysis of copy numbers was applied to all samples for selected loci. All target and reference assays were purchased from Applied Biosystems. RNaseP was used as endogenous control for normalization of analysed loci. The following assays were used: MTOR (Hs00873941), RB1 (Hs06406077), TP53 (Hs06423639), CDKN2A (Hs04369574), MYC (Hs03660964), SMAD4 (Hs06491600), FGFR1 (Hs00870416), TERT (Hs00412608), RICTOR (Hs01559952), PIK3CA (Hs06609754), MYCL (Hs00767289), MEN1 (Hs01778293), PTEN

(Hs05217581), CCND1 (Hs03772544), MET (Hs04951661), AKT1 (Hs2893205), FHIT (Hs03491211), SRC (Hs07169853) and RNaseP (part number 4403326). The experimental procedure recommended by the manufacturer (Applied Biosystems) was followed.

Fluorescent in situ hybridization (FISH) analysis on tumor samples.

A FISH analysis was developed according manufacturer instruction to validate CNV obtained by NGS analysis for the following genes: MYC, MDM2, ERBB2, CDKN2A, MET, TP53 and PTEN (all probes Vysis/Abbott Molecular) and RICTOR (Empire Genomics). Protocol, data analysis and interpretation were performed as previously reported [35, 36].

Western blotting and antibodies.

Immunoblotting was performed using the following antibodies in dilutions according manufacturer's recommendations, against Akt (#9272), phosphor-Akt(S473) (#4060), S6 (#2317), phospho-S6 (#4857), phospho-4E-BP1(#2855), β-Actin (#4967).

Expression analysis for genes of PI3K/mTOR pathway.

The Ion AmpliSeq Transcriptome Human Gene Expression Kit (Thermo Fisher) was used to analyse the expression levels of genes belonging to PI3K/mTOR family. To evaluate a potential correlation between RICTOR gene dosage and transcriptional output of PI3K/mTOR pathway, we applied a previously defined PI3K/mTOR transcriptional signature [37] and available dataset from MSigDB, which are based on genes that are modulated by PI3K inhibitors or involved in negative regulation of the pathway, respectively.

Statistical analysis.

Descriptive statistic was used to summarize pertinent study information. One-way ANOVA, Kruskal-Wallis test, Fisher's test with Monte Carlo simulation, and Fisher's exact test corrected for multiple comparisons were used as appropriate. The inter-rater variability and agreement between frequencies of both SM and CNV in training set and validation set was analyzed according to the Kappa (k) index. The index was interpreted according to the following values: <0.20 (bad); 0.21-0.40 (poor); 0.41-0.60 (moderate); 0.61-0.80 (good); and 0.81-1.00 (excellent) [38]. Correlation analysis between SM and CNV frequencies in training set and

validation set was also conducted, according to parametric (Pearson's r, with 95% confidence intervals, CI) and non-parametric (Spearman's Rho and Kendall's Tau) coefficients; a regression equation/line was calculated according to the regression analysis (parametric R2) [39]. In order to visually test and weigh differences between SM and CNV frequencies in training set and validation set, the Bland-Altman plots were determined [40]. For all the analyses, significance was defined at the $p<0.05$ level. The SPSS (v. 18.0), R (v. 3.2.1 and survival library v.2.38-2 for multivariate Cox regression) and MedCalc (v. 15.6) licensed statistical programs were used for all analyses.

RESULTS

Building of a clinical risk classification model for resected SQLC.

Patients.

Data from 573 patients from five different Italian institutions were gathered. Four hundred ninety-four patients were evaluable for the clinical analysis, with an attrition rate of 13.7%. Median age was 68 years (range: 32-83 years); the median number of resected nodes was 13 (range: 1-62). Overall patients' characteristics are shown in Table 1.

Table 1. Patients' characteristics (494 evaluable patients for the clinical analysis).

	Patients Number (%)
Gender	
Male	403 (81.6)
Female	91 (18.4)
T descriptor according to TNM 7th edition	
1	132 (26.7)
2	227 (46.0)
3	106 (21.6)
4	29 (5.7)
TNM staging	
I	259 (52.4)
II	118 (23.9)
III	102 (19.4)
IV	15 (2.4)
Lymph nodes	
Negative	339 (68.6)
Positive	155 (31.4)
Resected lymph nodes	
< 10	133 (26.9)
≥ 10	361 (73.1)
N status (N descriptor according to TNM 7th edition)	
0	339 (68.6)
1	65 (13.2)
2	63 (12.8)
3	27 (5.4)
Grading	
G 1-2	219 (44.3)
G 3	177 (35.9)
Unknown	98 (19.8)
Chemotherapy	
Neoadjuvant	26 (5.2)
Adjuvant	75 (15.2)
None	272 (55.1)
Unknown	121 (24.5)
Surgery	
Lobectomy	308 (62.3)
Bi-lobectomy	45 (9.1)
Pneumonectomy	74 (15.0)
Unknown	67 (13.6)

Survival analysis.

Median follow-up was 28 months (range: 1-213 months). The overall number of deaths was 202 (164 due to cancer, 38 due to other causes). Median DFS, CSS and OS were 38 months (95% CI 31-45), 81 months (95% CI 50-112) and 58 months (95% CI 42-74), with a 5-year rate of 38.6%, 55.8% and 48.6%, respectively. At the multivariate analysis, age ≤68 years, tumor size 1-2, negative nodes, and grading 1-2 were significant independent predictors for longer DFS and OS. With regard to CSS, tumor size 1-2, negative nodes, and grading 1-2 were significant prognostic predictors (Table 2).

Table 2. Multivariate survival analysis.

Variables	**DFS**			**CSS**			**OS**		
	HR	**95%CI**	***P***	**HR**	**95%CI**	***P***	**HR**	**95%CI**	***P***
Gender [male *versus* female]	-	-	-	-	-	-	-	-	-
Age [>68 *versus* ≤68 years]	1.58	1.14-2.18	*0.005*	-	-	-	2.17	1.48-3.17	*<0.0001*
T descriptor according to TNM 7th edition [3-4 *versus* 1-2]	1.75	1.22-2.51	*0.002*	2.26	1.40-3.66	*0.001*	2.12	1.40-3.21	*<0.0001*
Lymph nodes [positive *versus* negative]	2.27	1.57-3.27	*<0.0001*	2.93	1.79-4.80	*<0.0001*	2.59	1.70-3.96	*<0.0001*
Resected lymph nodes [<10 *versus* ≥10]	-	-	-	-	-	-	-	-	-
N status **(N** descriptor according to TNM 7th edition) [1 *versus* 0] [2-3 *versus* 0]	-	-	-	-	-	-	-	-	-
Grading [3 *versus* 1-2]	1.41	1.03-1.94	*0.033*	-	-	-	1.65	1.13-2.40	*0.008*
TNM staging (III/IV *versus* I/II)	-	-	-	-	-	-	-	-	-

Legend - Table 2: HR, hazard ratios; CI, confidence intervals.

Internal validation analysis.

At the cross-validation analysis, nodes, grading, tumor size and age were confirmed as independent factors for DFS (replication rate: 98%, 72%, 70% and 86%, respectively). The same factors were confirmed to be independent predictors for OS at the internal validation (replication rate: 100%, 98%, 100%, and 100% for nodes, grading, T-descriptor, and age, respectively). For what concerns CSS, at the cross-validation analysis nodes and T-descriptor were confirmed as independent predictors (replication rate: 93% and 93%, respectively).

Prognostic score and Model Performance.

According to the HRs obtained at the multivariate analysis, a prognostic scoring index was assigned to each patient to identify the individual risk of recurrence (Table 3).

Table 3. Prognostic score assessment according to Disease Free Survival.

Disease Free Survival	**Score points**		
	0	**1**	**2**
Age	≤68	>68	-
T-descriptor according to TNM 7th edition	1-2	-	3-4
Lymph nodes	Negative	-	Positive
Grading	1-2	3	-

The score dichotomization according to outcome, derived from the ROC analysis and the maximally selected log-rank statistics, identified 2 as the optimal cutoff point. According to the two-class model (model A), a statistically significant prognostic difference between patients at low (score ≤2) and high risk (score >2) was determined for both DFS (3-year: 64.6% and 32.4%, $p < 0.0001$; 5-year: 52.5% and 15.1%; $p < 0.0001$), CSS (3-year: 84.4% and 44.5%, $p < 0.0001$; 5-year: 78.8% and 24.5%; $p < 0.0001$), and OS (3-year: 77.3% and 38.8%, $p < 0.0001$; 5-year: 67.6% and 17.0%; $p < 0.0001$; Figure 1).

On the basis of the outcome, patients were divided into three risk classes, by considering cutoffs chosen at approximately equal distance along the range of values: (1) low risk of recurrence and death: score 0-2 (the best outcome estimate); (2) intermediate risk of recurrence and death: score 3-4; (3) high risk of recurrence and death: score 5-6 (worst outcome estimate). According to the three-class model (model B), a highly significant prognostic difference between patients at low, intermediate, and high risk was found for DFS (3-year: 64.6%, 39.8%, and 21.8%, $p < 0.0001$; 5-year: 52.5%, 23.2%, and 6.2%, $p < 0.0001$), CSS (3-year: 84.4%, 55.4%, and 30.9%, $p < 0.0001$; 5-year: 78.8%, 35.0%, and 15.5%, $p < 0.0001$), and OS (3-year: 77.3%, 47.9%, and 27.2%, $p < 0.0001$; 5-year: 67.6%, 25.4%, and 9.1%, $p < 0.0001$; Figure 1).

Figure 1. Disease Free Survival (A and B), Cancer Specific Survival (C and D) and Overall Survival (E and F), according to risk classes as developed for Model A (A, C and E) and Model B (B, D and F). The 5-years rate for each outcome is reported. p, P value at long-rank analysis.

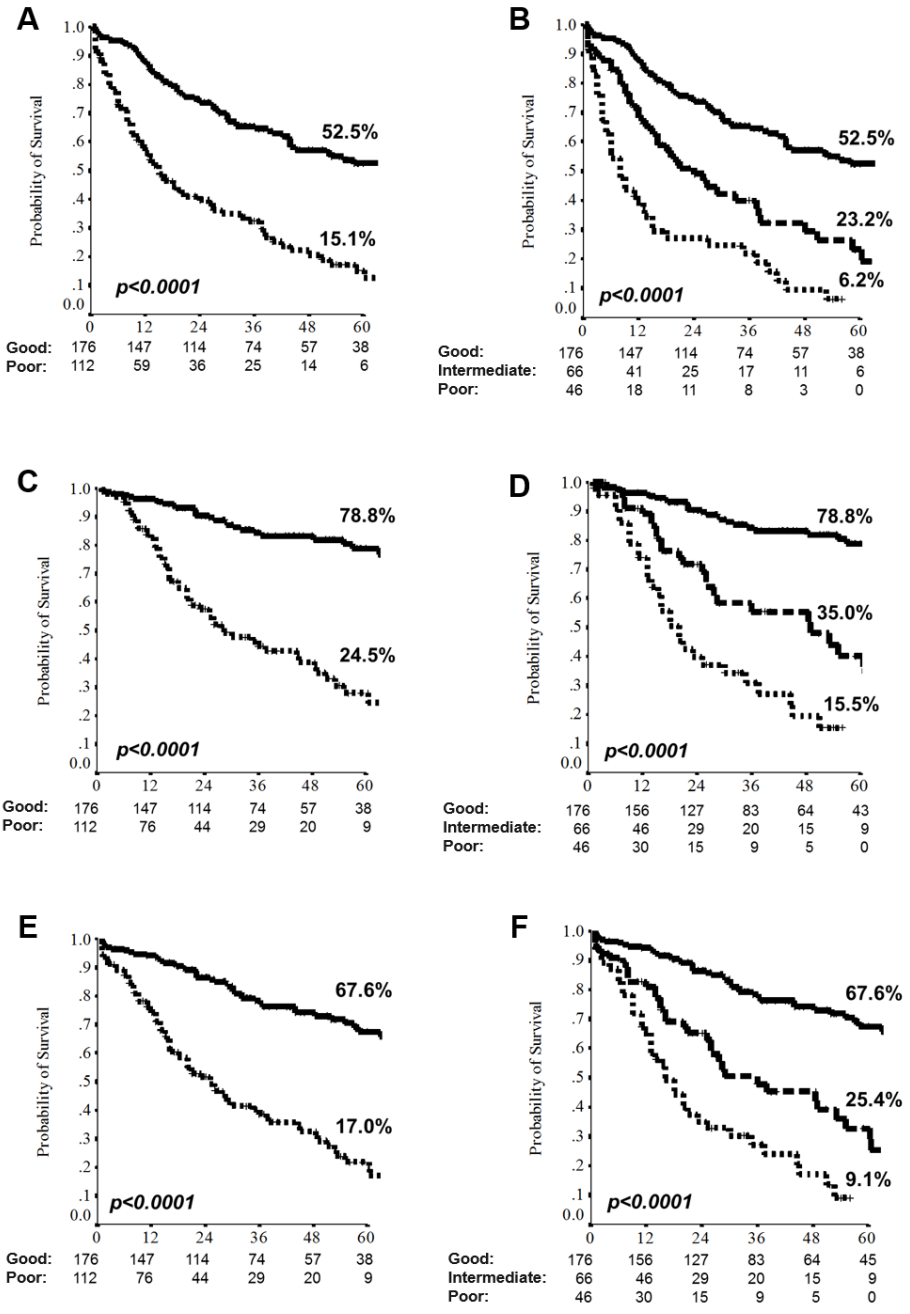

Validation of this clinical classification model in the context of an external cohort of resected SQLC.

Patients.

Data on 1,375 patients from six different Italian institutions were gathered. The patients' median age was 68 years (range 38-90 years). As a clinical descriptor, the median number of resected nodes was 17 (range 1-85). Patient characteristics are reported in Table 4. Most of the included patients were male (86.8%) and affected by SQLC with a T descriptor of 1 or 2 (71.7%) versus 3 or 4 (24.9%) and stage I or II (71%) versus III or IV (28.0%). Nearly half of the patients (46.3%) presented lymph node involvement. The most frequent surgical procedure among the included patients was lobectomy (67.1%), followed by pneumonectomy (24.9%). Overall, 384 patients (27.9%) were treated with adjuvant therapies, including platinum-based doublet chemotherapy (n = 254 [18.5%]), radiotherapy (n = 94 [6.8%]), and chemoradiotherapy (n = 36 [2.6%]). A total of 270 patients (19.6%) received neoadjuvant treatments, mainly platinum-based doublet chemotherapy (n = 254 [18.5%]), with only few cases of radiotherapy (n = 7 [0.5%]) and concomitant chemoradiotherapy (n = 9 [0.7%]). A total of 114 patients (8.3%) received both an adjuvant and a neoadjuvant treatment. According to the previously published prognostic model, 687 patients (50.0%) were classified as low-risk (score 0-2), 406 (29.5%) as intermediate-risk (score 3-4), and 123 patients (8.9%) as poor-risk (score 5-6) patients.

Table 4. Patients' characteristics (1,375 evaluable patients for the clinical analysis).

	Patients Number (%)
Median age (range)	68 (38-90)
Gender	
Male	1194 (86.8)
Female	181 (13.2)
Tumor size [T descriptor according to TNM 7th edition]	
0	22 (1.6)
1	300 (21.8)
2	686 (49.9)
3	255 (18.5)
4	88 (6.4)
Unknown	24 (1.7)
TNM staging	
I	555 (40.4)
II	421 (30.6)
III	376 (27.3)
IV	9 (0.7)
Unknown	14 (1.0)
Lymph nodes	
Negative	728 (52.9)
Positive	636 (46.3)
Unknown	11 (0.8)
Resected lymph nodes	
< 10	272 (19.8)
≥ 10	877 (63.8)
Unknown	226 (16.4)
N status [N descriptor according to TNM 7th edition]	
0	728 (52.9)
1	408 (29.7)
2	227 (16.5)
3	1 (0.1)
Unknown	11 (0.8)
Grading	
1-2	481 (35.0)
3	565 (41.1)
Unknown	329 (23.9)
Risk Class [according to the prognostic model]	
0-2	687 (50.0)
3-4	406 (29.5)
5-6	123 (8.9)
Unknown	159 (11.6)
Neoadjuvant Therapy	
No	934 (67.9)
Chemotherapy	254 (18.5)
Chemoradiotherapy	9 (0.7)
Radiotherapy	7 (0.5)
Unknown	171 (12.4)
Surgery	
Lobectomy	923 (67.1)
Bi-lobectomy	110 (8.0)
Pneumonectomy	342 (24.9)
Adjuvant Therapy	
No	728 (52.9)
Chemotherapy	254 (18.5)
Chemoradiotherapy	36 (2.6)
Radiotherapy	94 (6.8)
Unknown	263 (19.1)

Survival Analysis and Validation of the Prognostic Model.

The median follow-up calculated with the reverse method was 55 months (95% CI: 51–59). In all, 1,097 patients were evaluable for the survival analysis, with an attrition rate of 21.3% (the clinical or pathological descriptors for survival analysis were missing for 159 patients and the follow-up date was missing for 119 patients). According to the three-class model, patients included in the low-risk class had a significantly longer DFS than patients at intermediate (HR = 1.67, 95% CI: 1.40–2.01) and high risk (HR ¼ 2.46, 95% CI: 1.90–3.19). The 5-year DFS rates for low-, intermediate-, and high-risk patients were 51.0%, 33.5%, and 25.8%, respectively ($p < 0.0001$) (Figure 2A). In strict accordance, a statistically significant advantage was observed for low-risk patients versus for intermediate- and high-risk patients in terms of CSS (HR = 2.46, 95% CI: 1.80–3.36 versus HR = 4.30, 95% CI: 2.92–6.33) and OS (HR = 1.79, 95% CI: 1.48–2.17 versus HR ¼ 2.33, 95% CI: 1.76–3.07). The 5-year CSS rates for low-, intermediate-, and high-risk patients were 82.7%, 64.7%, and 53.3%, respectively ($p < 0.0001$). The 5-year OS rates for low, intermediate and high-risk patients were 56.7%, 37.9%, and 30.9%, respectively ($p < 0.0001$) (Figure 2B and C). The C-statistic values for DFS, CSS, and OS were 0.68 (95% CI: 0.63–0.73), 0.66 (95% CI: 0.61–0.71), and 0.68 (95% CI: 0.63–0.72), respectively.

Figure 2. Disease-free survival (A), cancer-specific survival (B), and overall survival (C) according to the three-class risk model. The 5-year rate for each outcome is reported; p value at long-rank analysis.

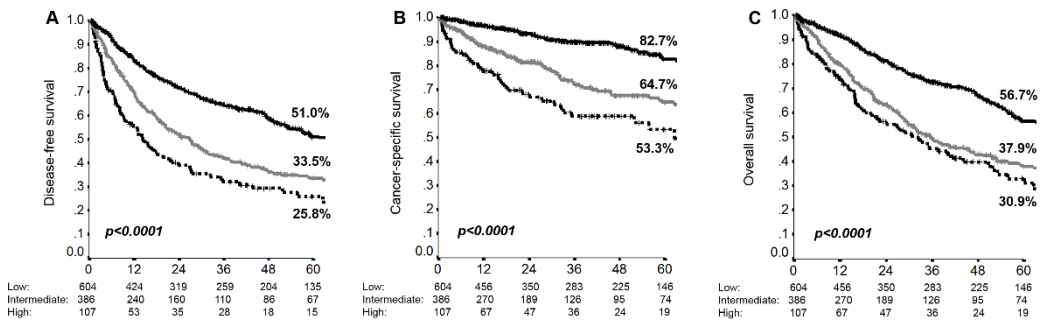

PS Analysis for the Impact of ANT.

In the entire patient cohort, no significant differences according to administration of ANT were observed in terms of DFS (p = 0.77 [5-year DFS 44.9% versus 42.8%]), CSS (p = 0.11 [5-year CSS 76.2% versus 67.4%]), or OS (p = 0.16 [5-year OS 52.0% versus 45.9%]) when the analysis was corrected by PS (Figure 3). Nevertheless, when the overall population was stratified according to the three-class risk model, a trend in favor of ANT was observed for intermediate-risk/high-risk patients, particularly in terms of CSS (p = 0.06 [5-year CSS 72.7% versus 60.8%]) (Figure 4). In the low-risk group, no significant differences according to the administration of ANT were observed in terms of any survival outcome analyzed.

Figure 3. Disease-free survival (A), cancer-specific survival (B), and overall survival (C) according to the administration of adjuvant and neoadjuvant treatment (ANT) in the overall population adjusted for propensity score analysis. The 5-year rate for each outcome is reported; p value at long-rank analysis.

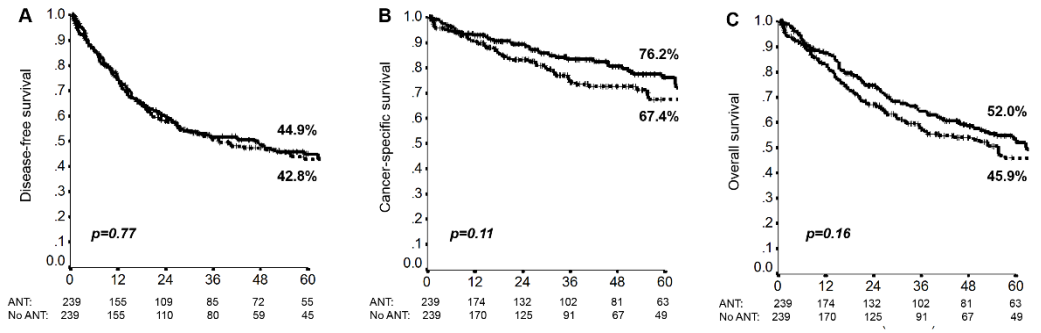

Figure 4. Disease-free survival (A), cancer-specific survival (B), and overall survival (C) according to the administration of adjuvant and neoadjuvant treatment (ANT) in the intermediate-risk/high-risk population adjusted for propensity score analysis. The 5-year rate for each outcome is reported; p value at long-rank analysis.

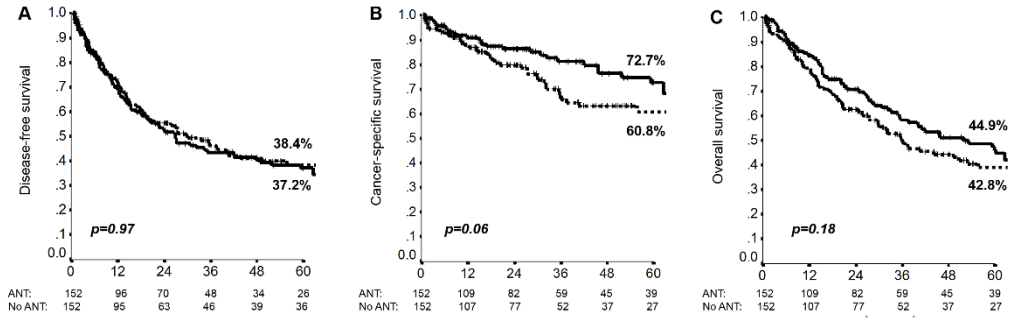

Analysis of the molecular portrait of prognostic outlier patients.

Patients' cohorts.

We conducted sequencing analyses on 60 resected SQLC samples (training set), 27 patients classified as GP and 33 as PP, according to the previously designed and validated three-class prognostic model. Training set patients' characteristics according to the prognostic groups are reported in Table 5.

Table 5. Clinical and pathological characteristics of the 60 patients included in the training set, separated in prognostic groups (PP and GP) according to the previously published three-class prognostic model.

Training Set	**PP (N = 33)**	**GP (N = 27)**
	Patient number (%)	
Median age [years]	74	63
Range	[67 - 82]	[43 - 72]
Gender		
Male	28 (84.8)	20 (74.0)
Female	5 (15.2)	7 (26.0)
TNM Staging [according to TNM 7th edition]		
I	0 (0.0)	14 (51.8)
II	0 (0.0)	13 (48.2)
III	33 (100.0)	0 (0.0)
Lymph nodes		
Negative	0 (0.0)	27 (100.0)
Positive	33 (100.0)	0 (0.0)
Tumor size [T descriptor according to TNM 7th edition]		
1	0 (0.0)	10 (33.3)
2	0 (0.0)	15 (59.3)
3	30 (78.8)	2 (7.4)
4	3 (21.2)	0 (0.0)
Node status [N descriptor according to TNM 7th edition]		
0	0 (0.0)	27 (100.0)
1	22 (36.4)	0 (0.0)
2	9 (51.5)	0 (0.0)
3	2 (12.1)	0 (0.0)
Grading		
1	0 (0.0)	3 (11.1)
2	5 (15.2)	20 (74.1)
3	28 (84.8)	4 (14.8)

Legend - Table 5. PP, poor prognosis; GP, good prognosis; N, number; NR, not reach.

An additional cohort of 37 specimens from resected SQLC patients, collected regardless of prognosis, was available as validation set from University of Perugia.

Molecular features.

In the training set, somatic mutations were detected in 59 cases in 38 genes (Figure 5A, Table 6). In detail, one mutation was observed in 9/60 cases (15.0%), more than one in 50/60 (83.3%) cases, while no alteration in only one case (1.7%). The most commonly mutated genes in the whole cohort was *TP53* (53/60; 88.3%) and *KMT2D* (10/60; 16.7%). CNV were observed in all cases in 40 genes (Figure 5B, Table 7]. In detail, one CNV was observed in 3/60 cases (5.0%), more than one in 57/60 cases (95.0%). CNV analysis showed copy number gain of *SOX2* (47/60; 78.3%) as the most frequent event, followed by gain in *PIK3CA* (34/60; 56.7%) and *TP63* (24/60; 40.0%). Of note, *RICTOR* gain was present in 14/60 samples (23.3%). An additional cohort of 37 resected SQLC samples was used to validate the molecular analysis results of the training set (Figure 5A-B).

Figure 5: Comparison of somatic mutations [A] and copy number variation [B] between training and validation set.

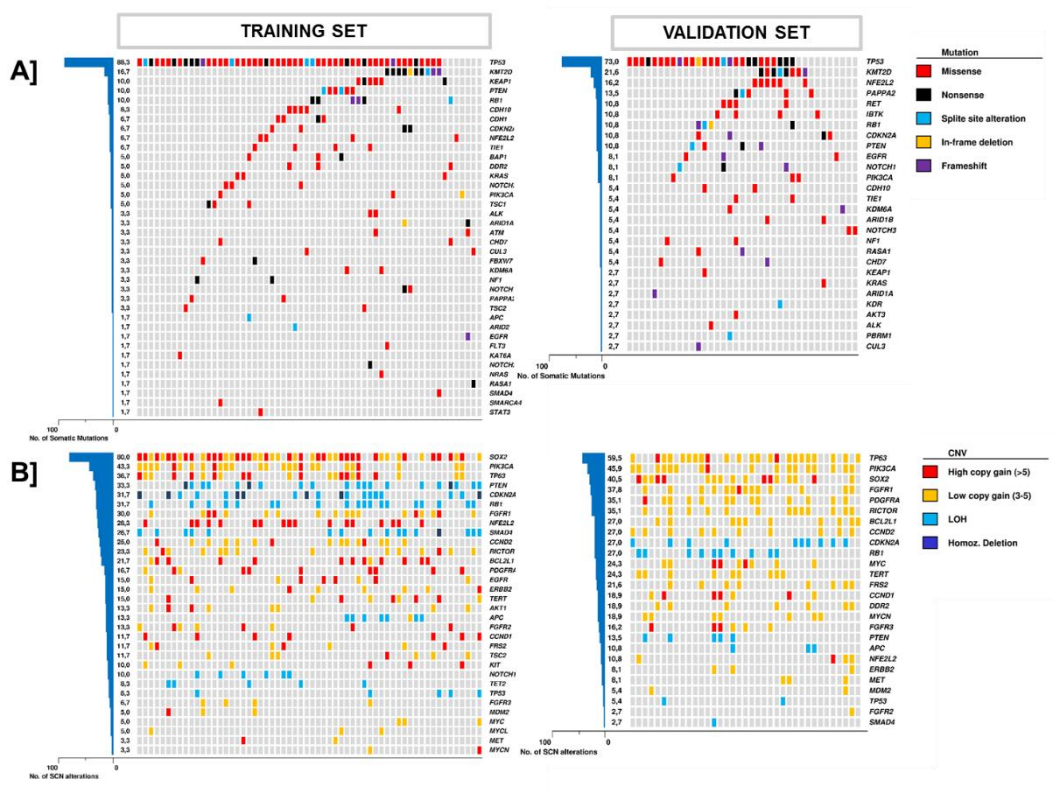

Legend - Figure 5: CNV, copy number variation; LOH, loss of heterozygosity.

Table 6. Prevalence of somatic mutations [SM] in 38 altered genes in 60 resected SQLC samples (training set) according to the prognostic groups (PP and GP).

Gene	PP N (%)	GP N (%)	Total N (%)	*p-value**
ALK	1 (3.0)	1 (3.7)	2 (3.3)	-
APC	0 (0.0)	1 (3.7)	1 (1.7)	-
ARID1A	1 (3.0)	1 (3.7)	2 (3.3)	-
ARID2	0 (0.0)	1 (3.7)	1 (1.7)	-
ATM	1 (3.0)	1 (3.7)	2 (3.3)	-
BAP1	1 (3.0)	2 (7.4)	3 (5.0)	-
CDH1	1 (3.0)	3 (11.1)	4 (6.7)	-
CDH10	1 (3.0)	4 (14.8)	5 (8.3)	-
CDKN2A	1 (3.0)	3 (11.1)	4 (6.7)	-
CHD7	1 (3.0)	1 (3.7)	2 (3.3)	-
CUL3	0 (0.0)	2 (7.4)	2 (3.3)	-
DDR2	0 (0.0)	3 (11.1)	3 (5.0)	-
EGFR	1 (3.0)	0 (0.0)	1 (1.7)	-
FBXW7	1 (3.0)	1 (3.7)	2 (3.3)	-
FLT3	1 (3.0)	0 (0.0)	1 (1.7)	-
KAT6A	1 (3.0)	0 (0.0)	1 (1.7)	-
KDM6A	1 (3.0)	1 (3.7)	2 (3.3)	-
KEAP1	4 (12.1)	2 (7.4)	6 (10.0)	-
KMT2D	7 (21.2)	3 (11.1)	10 (16.7)	-
KRAS	1 (3.0)	2 (7.4)	3 (5.0)	-
NF1	2 (6.1)	0 (0.0)	2 (3.3)	-
NFE2L2	1 (3.0)	3 (11.1)	4 (6.7)	-
NOTCH1	0 (0.0)	2 (7.4)	2 (3.3)	-
NOTCH2	1 (3.0)	0 (0.0)	1 (1.7)	-
NOTCH3	1 (3.0)	2 (7.4)	3 (5.0)	-
NRAS	1 (3.0)	0 (0.0)	1 (1.7)	-
PAPPA2	1 (3.0)	1 (3.7)	2 (3.3)	-
PIK3CA	3 (9.1)	0 (0.0)	3 (5.0)	-
PTEN	3 (9.1)	3 (11.1)	6 (10.0)	-
RASA1	0 (0.0)	1 (3.7)	1 (1.7)	-
RB1	2 (6.1)	4 (14.8)	6 (10.0)	-
SMAD4	1 (3.0)	0 (0.0)	1 (1.7)	-
SMARCA4	1 (3.0)	0 (0.0)	1 (1.7)	-
STAT3	0 (0.0)	1 (3.7)	1 (1.7)	-
TIE1	2 (6.1)	2 (7.4)	4 (6.7)	-
TP53	28 (84.8)	25 (92.6)	53 (88.3)	-
TSC1	1 (3.0)	2 (7.4)	3 (5.0)	-
TSC2	1 (3.0)	1 (3.7)	2 (3.3)	-

Legend - Table 6. N, number; p-value* are reported only if <0.05 according to Fisher's exact test.

Table 7. Prevalence of copy number variations [CNV] in 40 altered genes in 60 resected SQLC samples (training set) according to the prognostic groups (PP and GP).

Gene	PP N (%)	GP N (%)	Total N (%)	*p-value**
AKT1 [Gain]	3 (9.1)	2 (7.4)	5 (8.3)	-
APC [Loss]	3 (9.1)	3 (11.1)	6 (10.0)	-
BCL2L1 [Gain]	5 (15.2)	6 (22.2)	11 (18.3)	-
CCND1 [Gain]	5 (15.2)	4 (14.8)	9 (15.0)	-
CCND2 [Gain]	8 (24.2)	4 (14.8)	12 (20.0)	-
CDKN2A [Loss]	9 (27.3)	7 (25.9)	16 (26.7)	-
DDR2 [Gain]	3 (9.1)	3 (11.1)	6 (10.0)	-
EGFR [Gain]	4 (12.1)	4 (14.8)	8 (13.3)	-
ERBB2 [Gain]	5 (15.2)	3 (11.1)	8 (13.3)	-
FGFR1 [Gain]	5 (15.2)	6 (22.2)	11 (18.3)	-
FGFR2 [Gain]	3 (9.1)	4 (14.8)	7 (11.7)	-
FGFR3 [Gain]	2 (6.1)	3 (11.1)	5 (8.3)	-
FOXP1 [Loss]	7 (21.2)	10 (37.0)	17 (28.3)	-
FOXP4 [Loss]	2 (6.1)	4 (14.8)	6 (10.0)	-
FRS2 [Gain]	7 (21.2)	5 (18.5)	12 (20.0)	-
JAK3 [Gain]	6 (18.2)	6 (22.2)	12 (20.0)	-
KIT [Gain]	4 (12.1)	1 (3.7)	5 (8.3)	-
MCL1 [Gain]	9 (27.3)	5 (18.5)	14 (23.3)	-
MDM2 [Gain]	6 (18.2)	6 (22.2)	12 (20.0)	-
MET [Gain]	2 (6.1)	1 (3.7)	3 (5.0)	-
MYC [Gain]	3 (9.1)	1 (3.7)	4 (6.7)	-
MYCL1 [Gain]	2 (6.1)	2 (7.4)	4 (6.7)	-
MYCN [Gain]	2 (6.1)	2 (7.4)	4 (6.7)	-
NFE2L2 [Gain]	6 (18.2)	1 (3.7)	7 (11.7)	-
NOTCH1 [Loss]	4 (12.1)	1 (3.7)	5 (8.3)	-
PBRM1 [Loss]	7 (21.2)	7 (25.9)	14 (23.3)	-
PDGFRA [Gain]	5 (15.2)	5 (18.5)	10 (16.7)	-
PIK3CA [Gain]	18 (54.5)	16 (59.3)	34 (56.7)	-
PTCH1 [Loss]	5 (15.2)	2 (7.4)	7 (11.7)	-
PTEN [Loss]	11 (33.3)	10 (37.0)	21 (35.0)	-
RB1 [Loss]	9 (27.3)	6 (22.2)	15 (25.0)	-
RICTOR [Gain]	7 (21.2)	7 (25.9)	14 (23.3)	-
SMAD4 [Loss]	11 (33.3)	2 (7.4)	13 (21.7)	*0.025*
SMARCB1 [Gain]	7 (21.2)	8 (29.6)	15 (25.0)	-
SOX2 [Gain]	24 (72.7)	23 (85.2)	47 (78.3)	-
TERT [Gain]	6 (18.2)	3 (11.1)	9 (15.0)	-
TET2 [Loss]	1 (3.0)	3 (11.1)	4 (6.7)	-
TP53 [Loss]	2 (6.1)	2 (7.4)	4 (6.7)	-
TP63 [Gain]	14 (42.4)	10 (37.0)	24 (40.0)	-
TSC2 [Gain]	1 (3.0)	-	1 (1.7)	-

Legend - Table 6. N, number; *p-value** are reported only if *<0.05* according to Fisher's exact test.

Comparison between the two cohorts is reported in Figure 6A-B. A substantial agreement for SM and CNV frequencies in training and validation set was observed, with a significant overall correlation between them (Figure 6C). The Bland-Altman plot did confirm the absence of major differences or discrepancies between SM and CNV frequencies in training and validation set (Figure 6D).

Figure 6: Frequencies of somatic mutations, SM [A] and copy number variations, CNV [B] in training (TS) and validation set (VS). Inter-agreement weighted K, correlation and regression analysis SM and CNV frequencies between TS and VS according to Pearson, Spearman and Kendall-Thau's tests [C]. Bland-Altman plot weighting differences in SM and CNV frequencies between TS and VS [differences plotted against TS] [D].

A]

SM	Training Set (TS)		Validation Set (VS)	
Gene	60	%	37	%
ALK	2	3,3	1	2,7
APC	1	1,7	0	0,0
ARID1A	2	3,3	1	2,7
ARID2	1	1,7	0	0,0
ATM	2	3,3	0	0,0
BAP1	3	5,0	0	0,0
CDH1	4	6,7	0	0,0
CDH10	5	8,3	2	5,4
CDKN2A	4	6,7	4	10,8
CHD7	2	3,3	2	5,4
CUL3	2	3,3	1	2,7
DDR2	3	5,0	0	0,0
EGFR	1	1,7	3	8,1
FBXW7	2	3,3	0	0,0
FLT3	1	1,7	0	0,0
KAT6A	1	1,7	0	0,0
KDM6A	2	3,3	2	5,4
KEAP1	6	10,0	1	2,7
KMT2D	10	16,7	8	21,6

SM	Training Set (TS)		Validation Set (VS)	
Gene	60	%	37	%
KRAS	3	5,0	1	2,7
NF1	2	3,3	2	5,4
NFE2L2	4	6,7	6	16,2
NOTCH1	2	3,3	3	8,1
NOTCH2	1	1,7	0	0,0
NOTCH3	3	5,0	2	5,4
NRAS	1	1,7	0	0,0
PAPPA2	2	3,3	5	13,5
PIK3CA	3	5,0	3	8,1
PTEN	6	10,0	4	10,8
RASA1	1	1,7	2	5,4
RB1	6	10,0	4	10,8
SMAD4	1	1,7	0	0,0
SMARCA4	1	1,7	0	0,0
STAT3	1	1,7	0	0,0
TIE1	4	6,7	2	5,4
TP53	53	88,3	27	73,0
TSC1	3	5,0	0	0,0
TSC2	2	3,3	0	0,0

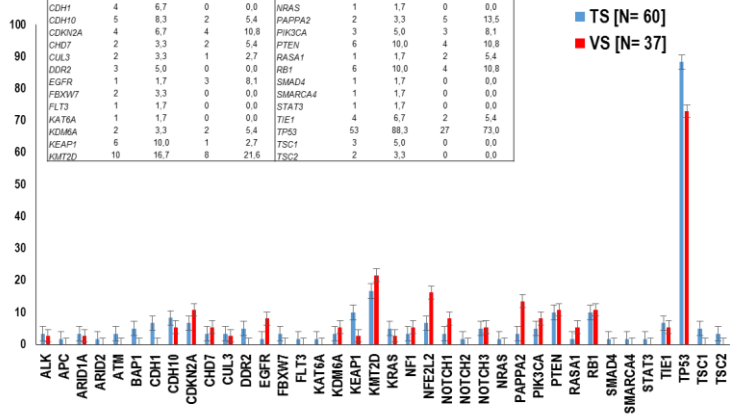

B]

CNV	Training Set (TS)		Validation Set (VS)	
Gene	60	%	37	%
AKT1 [Gain]	5	8,3	6	16,2
APC [Loss]	6	10,0	4	10,8
BCL2L1 [Gain]	11	18,3	10	27,0
CCND1 [Gain]	9	15,0	7	18,9
CCND2 [Gain]	12	20,0	10	27,0
CDKN2A [Loss]	16	26,7	10	27,0
EGFR [Gain]	8	13,3	3	8,1
ERBB2 [Gain]	8	13,3	3	8,1
FGFR1 [Gain]	11	18,3	8	21,6
FGFR2 [Gain]	7	11,7	1	2,7
FGFR3 [Gain]	5	8,3	6	16,2
FRS2 [Gain]	12	20,0	8	21,6
MDM2 [Gain]	12	20,0	8	21,6
MET [Gain]	3	5,0	3	8,1
MYC [Gain]	4	6,7	3	8,1

CNV	Training Set (TS)		Validation Set (VS)	
Gene	60	%	37	%
MYCL [Gain]	4	6,7	0	0,0
NFE2L2 [Gain]	7	11,7	4	10,8
NOTCH1 [Loss]	5	8,3	0	0,0
PIK3CA [Gain]	34	56,7	17	45,9
PTEN [Loss]	21	35,0	5	13,5
RB1 [Loss]	15	25,0	10	27,0
RICTOR [Gain]	14	23,3	13	35,1
SMAD4 [Loss]	13	21,7	1	2,7
SOX2 [Gain]	47	78,3	24	64,9
TERT [Gain]	9	15,0	9	24,3
TET2 [Loss]	4	6,7	0	0,0
TP53 [Loss]	4	6,7	2	5,4
TP63 [Gain]	24	40,0	23	62,2
TSC2 [Gain]	1	1,7	0	0,0

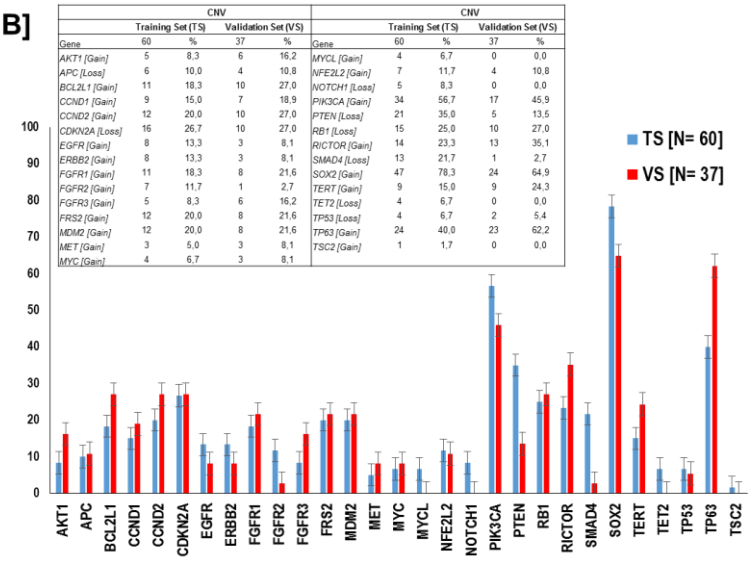

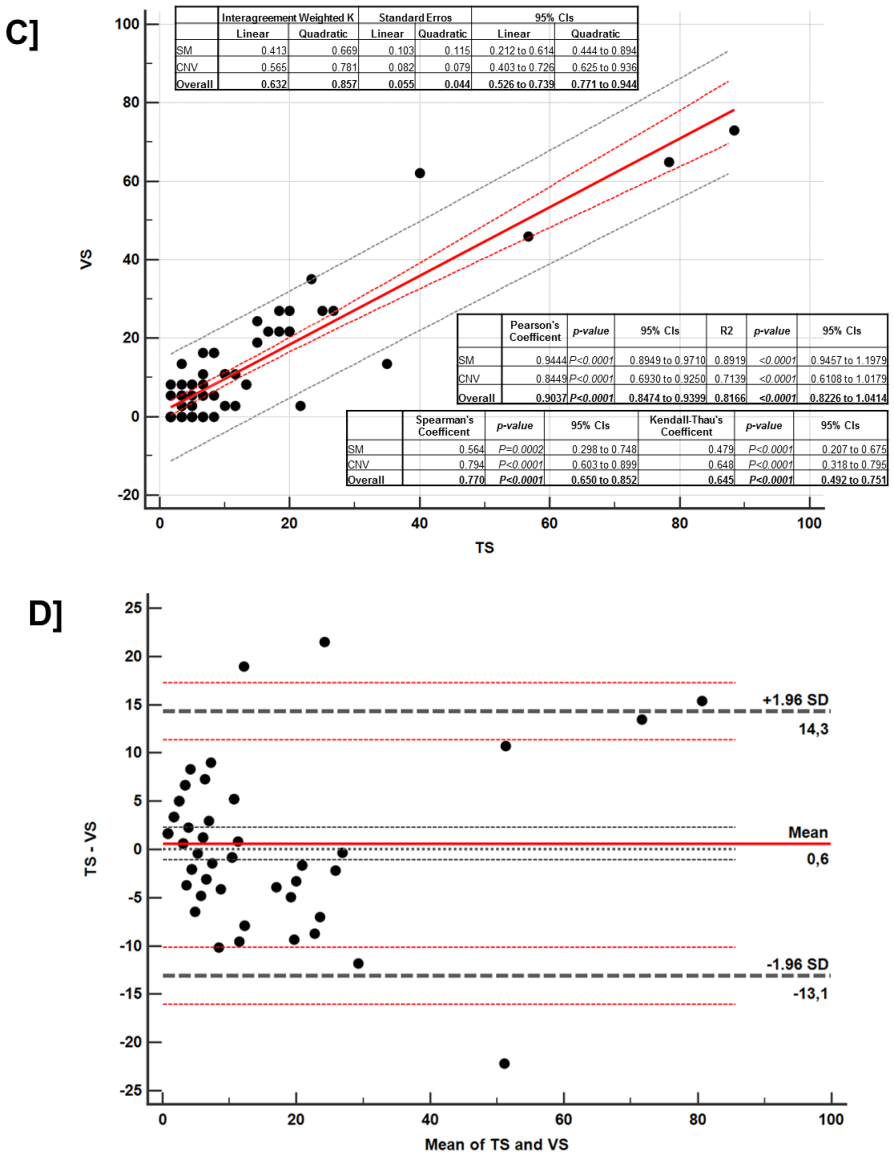

Legend - Figure 6: TS, training set; VS, validation set; N, number; SM, somatic mutation; CNV, copy number variation; CI, confidence interval.

In order to characterize the molecular background of SQLC prognostic outliers, we stratified the training cohort according to the prognostic model. A significant prognostic difference between patients at good and poor prognosis was found for disease-free survival (3-year: 42.9% and 10.4%, p=0.003), cancer-specific survival (3-year: 72.3% and 34.1%, p=0.02) and overall survival (3-year: 69.3% and 35.8%, p=0.01) (Figure 7).

Figure 7: Disease-free survival, cancer-specific survival and overall survival for good (GP) [blue line] and poor (PP) prognosis [yellow line] groups according to the published risk model. The 3-year rate for each outcome is reported, p value at long-rank analysis.

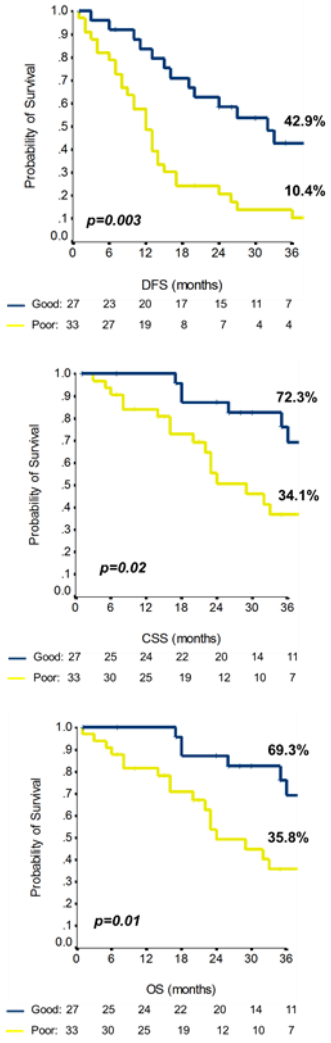

Legend - Figure 7: Disease-free survival, DFS; cancer-specific survival, CSS; overall survival, OS.

The prevalence of SM and CNV according to prognostic groups are reported in Figure 8. In 33 cases of the PP group, *TP53* was the most mutated gene (28/33; 84.8%), followed by *KMT2D* (7/33; 21.2%) and *KEAP1* (4/33; 12.1%). Interestingly, *PIK3CA* (3/33; 9.1%) and *NF1* (2/33; 6.1%) were mutated at low frequency, but exclusively in PP group. Regarding CNV, copy number gain in *SOX2* (24/33; 72.7%) was the most frequent event, followed by *PIK3CA* gain (18/33; 54.5%). *SMAD4* loss was particularly enriched in PP compared with GP

group (11/33; 33.3% versus 2/27; 7.4%, p=0.025), resulting in a statistically significant higher chance to be associated with poor prognosis (OR 4.491, 95% CI 1.320 - 15.277, p=0.016) (Figure 8). In the 27 patients of the GP group, *TP53* was the most mutated gene (25/27; 92.6%), followed by *CDH10* and *RB1* (4/27; 14.8%). *DDR2* mutations were exclusively identified in GP group (3/27; 11.1%) with a higher possibility to be associated with good prognosis (OR 0.100, 95%CI 0.010 - 1.014, p=0.051) (Figure 8). About CNV, GP shared with PP a similar frequency in term of gain in *SOX2* (12/33; 36.4%), *PIK3CA* (16/27; 59.3%) and *TP63* (10/27; 37.0%). Other frequent events observed included *FOXP1* and *PTEN* loss (10/27; 37.0%).

Figure 8. Comparison of mutational load, chromosome integrity number, somatic mutations and copy number variation between PP and GP. Blue columns and green columns represent SM and CNV, respectively. Odds Ratio analysis of somatic mutations and copy-number variation according to prognosis: an OR<1 indicates a higher chance to be associated with good prognosis; an OR>1 indicates a higher chance to be associated with poor prognosis.

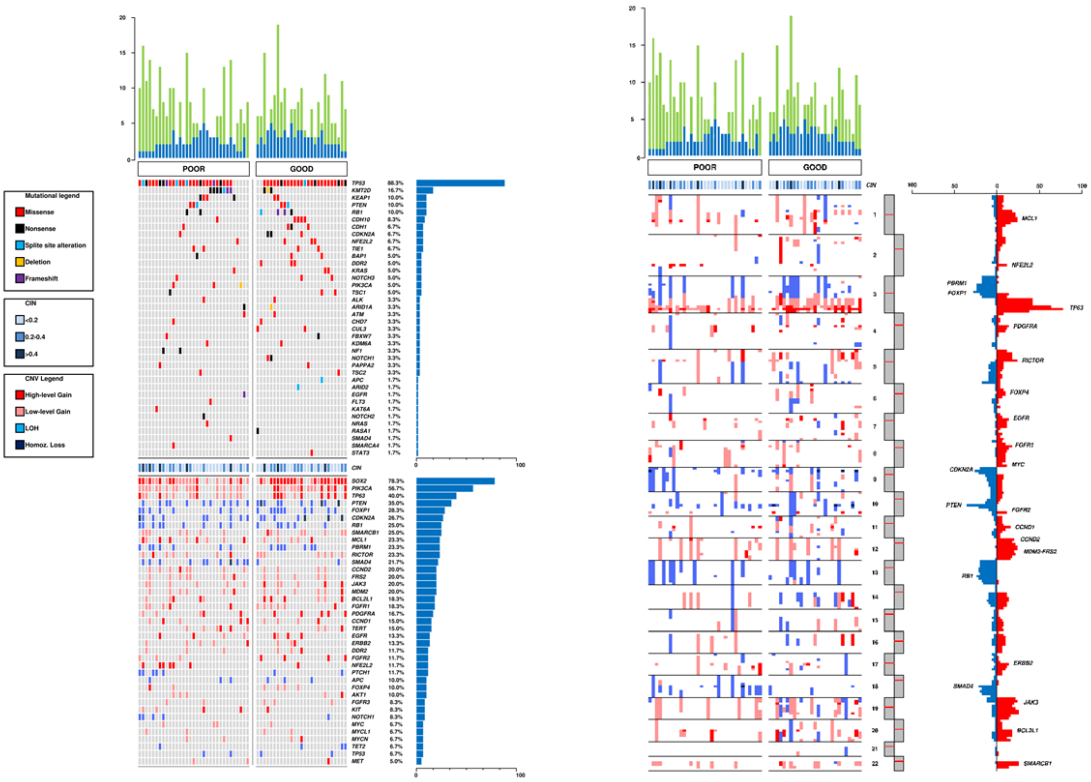

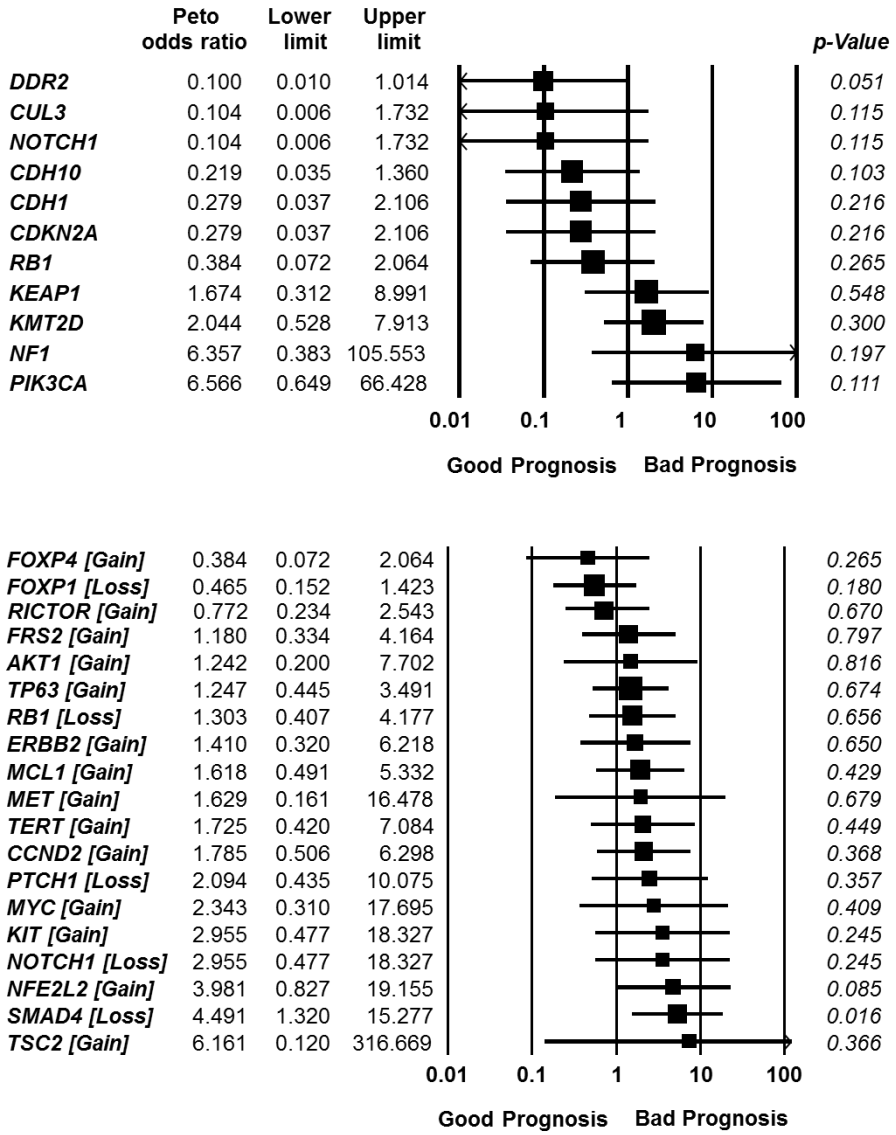

Legend - Figure 8: CIN, chromosome integrity number; CNV, copy number variation; OR, Odds Ratio; CI, confidence interval; SM, somatic mutation.

Tumor Mutational Burden (TMB) was estimated according to Rizvi et al.9 using the 1.7 Mb of genomic space covered by the CCP. A global median of 1.2 mutations/Mb (1.4 mean) was achieved for all samples analyzed. In particular, in PP group a median of 1.2 mutations/Mb (1.2 mean) was observed, while in GP group a median of 1.8 mutations/Mb (1.6 mean) (Figure 9).

Figure 9: Tumor Mutation Burden analysis according to prognosis.

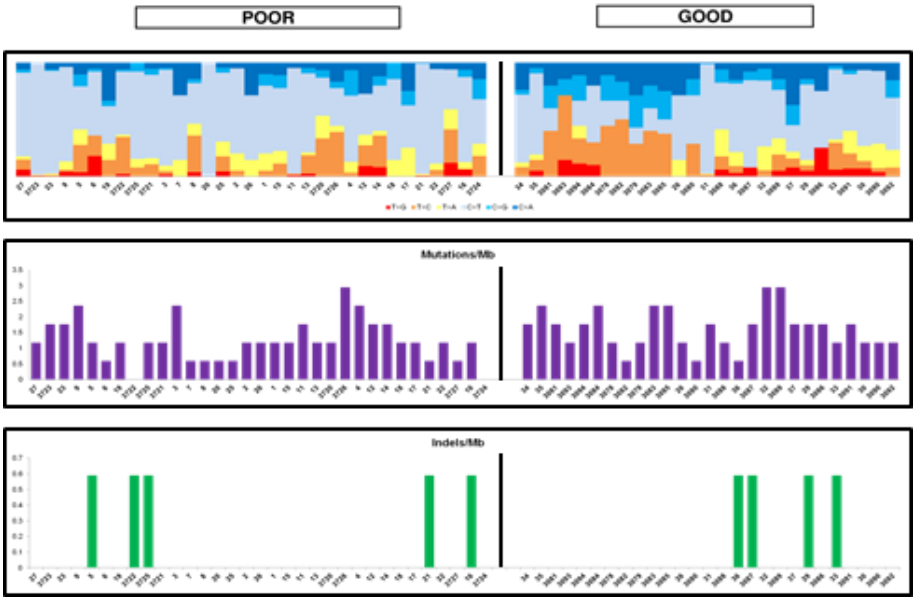

Although no significant difference according to the prognosis emerged in term of alterations of the mTOR family members, PI3KCA mutations and RICTOR high gain amplification were detected only in PP group (Figure 10). Overall, alterations in genes involved in the PI3K/mTOR pathway were detected in 42% of the analysed samples.

Figure 10. Prevalence of mTOR pathways alterations in GP and PP groups.

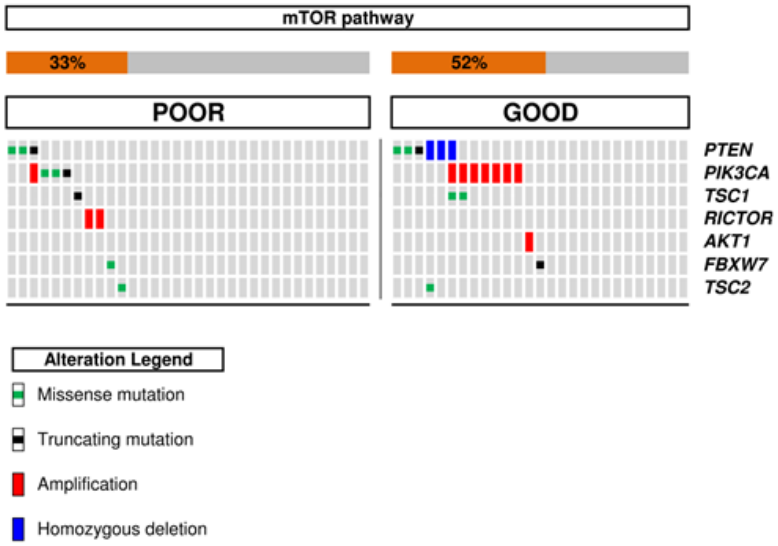

Transcriptomic analysis of PI3K/mTOR pathway.

Looking for a possible correlation between *RICTOR* gene dosage and transcriptional output of PI3K/mTOR pathway, in our cohort we found a trend for a positive correlation between the PI3K signature and high gain of *RICTOR* (Figure 11A). In keeping with this, we found an inverse correlation between high gain of *RICTOR* and a signature of negative regulators of the pathway, which might suggest increased pathway activity (Figure 11B).

Figure 11. Transcriptional signatures of PI3K/mTOR activation in SQLC. Higher levels of the PI3K signature (lPMID Creighton) in *RICTOR* high gain cases (HG, n=2) compared to *RICTOR* low gain (LG, n=10) and *RICTOR* wild-type (WT, n=26) [A]. Lower levels of the "Negative regulation of the PI3K AKT Network" signature in *RICTOR* high gain cases (HG, n=2) compared to *RICTOR* low gain (LG, n=10) and *RICTOR* wild-type (WT, n=26) [B]. Box plot represents the lower, median and upper quartile, while whiskers represent the highest and the lowest range for the upper and lower quartiles.

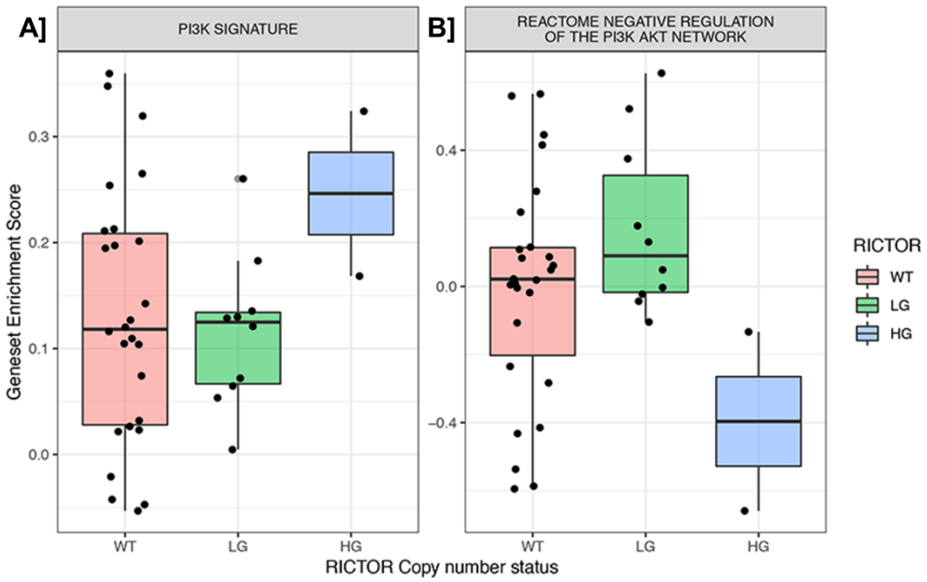

The mTOR pathway analysis was further performed subdividing the interacting partners in five blocks (Figure 12): i) activators/repressors of mTORC1; ii) exclusive partners of mTORC1; iii) common partners of mTORC1 and mTORC2; iv) exclusive partners of mTORC2; v) RICTOR interacting factors.

Figure 12. Gene expression levels of upstream activators/repressors of mTORC1 [A], exclusive partners of mTORC1 complex [B], common partners of mTORC1 and mTORC2 complex [C], exclusive partners of mTORC2 complex [D], exclusive partners of RICTOR outside of the mTORC2 complex [E]. Transcript levels are expressed as normalized counts per million.

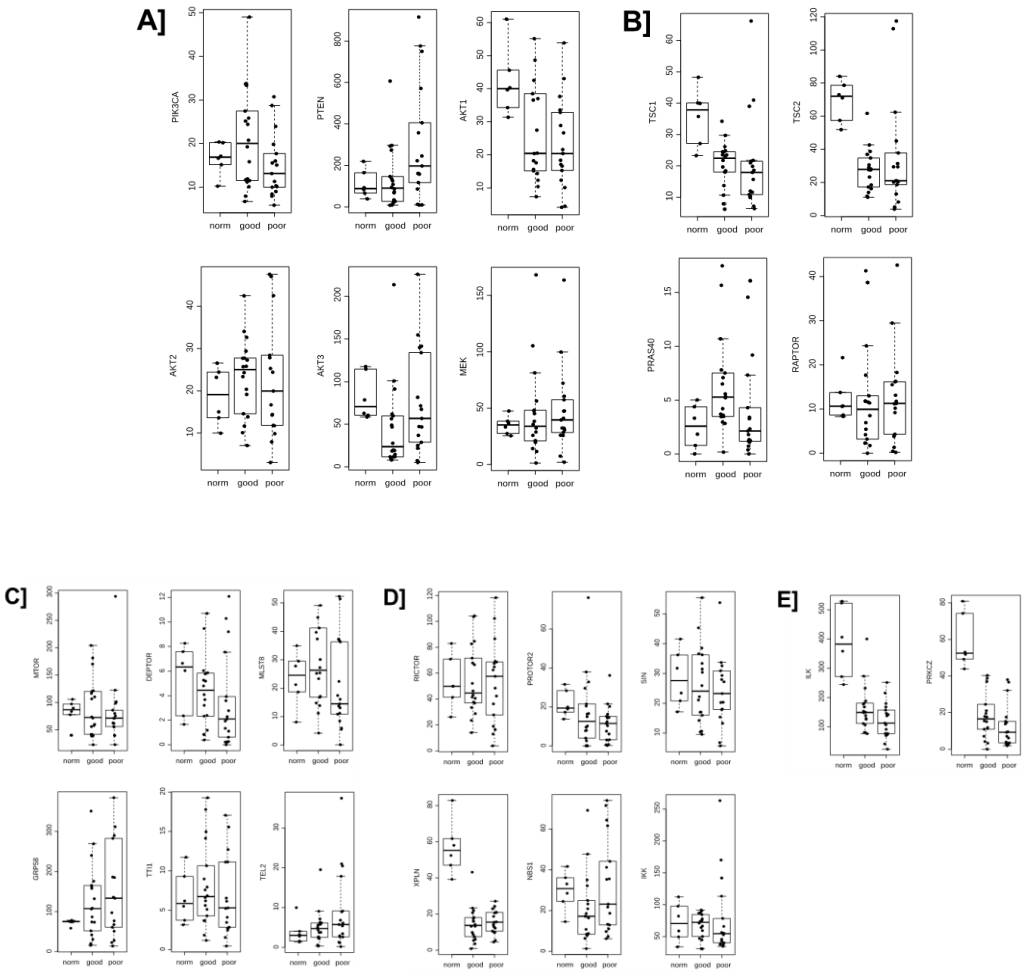

DISCUSSION

In the era of cancer molecular profiling, the design and application of risk models based on clinical parameters still provides valuable information for clinicians. Moreover, the abundance of genomic analyses did not always translate into a clinically meaningful result. Therefore, the most promising approach is likely to be represented by an integration of clinical data and genomic-proteomic characterization. The results of this study support the strength of an integrative approach, extending from prognostic dichotomization to multi-platform genomic/transcriptomic analyses, able to unravel candidate aberrations with a biological impact on SQLC oncogenesis.

The most intriguing finding we obtained concerns the validation of the PI3K/mTORC2-RICTOR axis as a crucial signalling pathway for SQLC in term of prevalence and druggable potential. In this regard, we observed alterations in genes involved in the mTOR pathway in 42% of training set samples, consistent with the reported 47% by TGCA [10]. Although after dichotomizing the patients in prognostic subgroups no significant correlations with molecular alterations emerged, interestingly *PI3KCA* mutations and *RICTOR* high gain were detected only in PP group. These observations, together with emerging evidence suggesting the interpretation of PI3K/mTOR pathway not only as a unique entity but partitioning it into its distinct mTORC1/2-defining subunits and interactors, led our study towards a deeper investigation of mTOR pathway [41]. In contrast with mTORC1, the mTORC2 still represents a structure with multiple unexplored aspects that require convincing answers. Among its components, RICTOR has an indispensable role with constantly increasing data implicating its aberrant overexpression across numerous cancer types [42]. The molecular analysis of overall training set identified *RICTOR* copy number gain in 23.3%, similarly to TGCA (16%)., Furthermore, the transcriptome analysis suggested that *RICTOR* high gain patients presented an increased PI3K/mTOR pathway activity, reinforcing the oncogenic background of RICTOR. The identification and validation of a reliable biomarker mirroring clinically meaningful PI3K/mTOR/Akt inhibition represents a compulsory aim in lung cancer. However, clinical trials exploring the efficacy of numerous PI3K/mTOR inhibitors did not conclude to solid benefit,

particularly in the context of unselected patients [43]. With this final aim, based on our molecular and transcriptomic findings, we designed a series of preclinical studies based on *RICTOR*-amplified SQLC *in vitro* models that are currently ongoing.

Dealing with prognosis, it has to be considered that the prognostic impact of a biomarker is not always associated with its predictive value. Exemplificative the case of ERCC1 in lung cancer, where a high *ERCC1* expression is associated with an improved survival, but a worst outcome after cisplatin-based adjuvant chemotherapy [44]. Focusing on the two molecular alterations that stratified according to prognosis, *DDR2* mutations were detected in 5% of our cohort, similarly with what was previously described [45]. Of interest, while to date no correlation between *DDR2* mutations and survival has been reported [46], we observed a significant trend for improved survival in *DDR2* mutant patients, all belonging to GP group. By contrary, *SMAD4* loss was statistically significantly associated with a worse prognosis (33.3% in PP versus 7.4% in GP) and this is the first evidence in lung cancer, in line with other diseases where this alteration was more widely explored [47]. In light of the suggested increased sensitivity to DNA topoisomerase inhibitors in lung cancer, this prognostic implication is highly intriguing for further investigations [48].

In the era of immunotherapy, TMB represents a candidate predictive biomarker. Our preliminary findings generated by NGS, described a higher TMB in GP than in PP group, contributing to enrich the prognostic speculations that are still debatable [49, 50].

CONCLUSION

In conclusions, our multi-step genomic analysis performed in almost 100 samples allowed to obtain a representative picture of SQLC molecular status according to patients' prognosis and to identify altered pathways with a biological impact in SQLC oncogenesis, as the PI3K/mTORC2-RICTOR axis. Planning to explore the potential role of RICTOR as a predictive biomarker in the context of *in vitro* and *in vivo* studies and early clinical trial, the existence of an extensive cross talk and concomitant aberrations in other genetic loci (KRAS, BRAF) in patients with PI3K/mTOR alterations needs to be considered. In fact, in clinical setting this factor might sabotage the monotherapy targeting through feedback loops, proposing the idea of a combinatorial treatment approach.

The introduction and validation of a personalized approach in the context of SQLC might allow the clinicians to provide the best available therapy for every individual patient to potentiate the expected clinical benefit and reduce the human and economic cost resulting from a less efficacious not-targeted treatment.

REFERENCES

1. Barlesi F, Mazieres J, Merlio JP et al. Routine molecular profiling of patients with advanced non-small-cell lung cancer: results of a 1-year nationwide programme of the French Cooperative Thoracic Intergroup (IFCT). Lancet 2016; 387: 1415-1426.
2. Maemondo M, Inoue A, Kobayashi K et al. Gefitinib or chemotherapy for non-small-cell lung cancer with mutated EGFR. N Engl J Med 2010; 362: 2380-2388.
3. Mitsudomi T, Morita S, Yatabe Y et al. Gefitinib versus cisplatin plus docetaxel in patients with non-small-cell lung cancer harbouring mutations of the epidermal growth factor receptor (WJTOG3405): an open label, randomised phase 3 trial. Lancet Oncol 2010; 11: 121-128.
4. Rosell R, Carcereny E, Gervais R et al. Erlotinib versus standard chemotherapy as first-line treatment for European patients with advanced EGFR mutation-positive non-small-cell lung cancer (EURTAC): a multicentre, open-label, randomised phase 3 trial. Lancet Oncol 2012; 13: 239-246.
5. Peters S, Camidge DR, Shaw AT et al. Alectinib versus Crizotinib in Untreated ALK-Positive Non-Small-Cell Lung Cancer. N Engl J Med 2017; 377: 829-838.
6. Shaw AT, Kim DW, Nakagawa K et al. Crizotinib versus chemotherapy in advanced ALK-positive lung cancer. N Engl J Med 2013; 368: 2385-2394.
7. Goldstraw P, Chansky K, Crowley J et al. The IASLC Lung Cancer Staging Project: Proposals for Revision of the TNM Stage Groupings in the Forthcoming (Eighth) Edition of the TNM Classification for Lung Cancer. J Thorac Oncol 2016; 11: 39-51.
8. Travis WD, Brambilla E, Riely GJ. New pathologic classification of lung cancer: relevance for clinical practice and clinical trials. J Clin Oncol 2013; 31: 992-1001.
9. Tsuta K, Kawago M, Inoue E et al. The utility of the proposed IASLC/ATS/ERS lung adenocarcinoma subtypes for disease prognosis and correlation of driver gene alterations. Lung Cancer 2013; 81: 371-376.
10. Cancer Genome Atlas Research N. Comprehensive genomic characterization of squamous cell lung cancers. Nature 2012; 489: 519-525.
11. Herbst RS, Gandara DR, Hirsch FR et al. Lung Master Protocol (Lung-MAP)-A Biomarker-Driven Protocol for Accelerating Development of Therapies for Squamous Cell Lung Cancer: SWOG S1400. Clin Cancer Res 2015; 21: 1514-1524.
12. Alexandrov LB, Nik-Zainal S, Wedge DC et al. Signatures of mutational processes in human cancer. Nature 2013; 500: 415-421.

13. Tsao MS, Le Teuff G, Shepherd FA et al. PD-L1 protein expression assessed by immunohistochemistry is neither prognostic nor predictive of benefit from adjuvant chemotherapy in resected non-small cell lung cancer. Ann Oncol 2017; 28: 882-889.
14. Kummar S, Williams PM, Lih CJ et al. Application of molecular profiling in clinical trials for advanced metastatic cancers. J Natl Cancer Inst 2015; 107.
15. Iasonos A, Schrag D, Raj GV, Panageas KS. How to build and interpret a nomogram for cancer prognosis. J Clin Oncol 2008; 26: 1364-1370.
16. Alonzo TA. Standards for reporting prognostic tumor marker studies. J Clin Oncol 2005; 23: 9053-9054.
17. Simon RM, Paik S, Hayes DF. Use of archived specimens in evaluation of prognostic and predictive biomarkers. J Natl Cancer Inst 2009; 101: 1446-1452.
18. Shuster JJ. Median follow-up in clinical trials. J Clin Oncol 1991; 9: 191-192.
19. Hess KR. Graphical methods for assessing violations of the proportional hazards assumption in Cox regression. Stat Med 1995; 14: 1707-1723.
20. Bria E, Milella M, Sperduti I et al. A novel clinical prognostic score incorporating the number of resected lymph-nodes to predict recurrence and survival in non-small-cell lung cancer. Lung Cancer 2009; 66: 365-371.
21. Pencina MJ, D'Agostino RB. Overall C as a measure of discrimination in survival analysis: model specific population value and confidence interval estimation. Stat Med 2004; 23: 2109-2123.
22. Hanley JA, McNeil BJ. The meaning and use of the area under a receiver operating characteristic (ROC) curve. Radiology 1982; 143: 29-36.
23. Di Maio M, Lama N, Morabito A et al. Clinical assessment of patients with advanced non-small-cell lung cancer eligible for second-line chemotherapy: a prognostic score from individual data of nine randomised trials. Eur J Cancer 2010; 46: 735-743.
24. Bria E, De Manzoni G, Beghelli S et al. A clinical-biological risk stratification model for resected gastric cancer: prognostic impact of Her2, Fhit, and APC expression status. Ann Oncol 2013; 24: 693-701.
25. Efficace F, Bottomley A, Smit EF et al. Is a patient's self-reported health-related quality of life a prognostic factor for survival in non-small-cell lung cancer patients? A multivariate analysis of prognostic factors of EORTC study 08975. Ann Oncol 2006; 17: 1698-1704.

26. Sauerbrei W, Schumacher M. A bootstrap resampling procedure for model building: application to the Cox regression model. Stat Med 1992; 11: 2093-2109.
27. Harrell FE, Jr., Lee KL, Califf RM et al. Regression modelling strategies for improved prognostic prediction. Stat Med 1984; 3: 143-152.
28. Travis WD, Brambilla E, Nicholson AG et al. The 2015 World Health Organization Classification of Lung Tumors: Impact of Genetic, Clinical and Radiologic Advances Since the 2004 Classification. J Thorac Oncol 2015; 10: 1243-1260.
29. Goldstraw P, Crowley J, Chansky K et al. The IASLC Lung Cancer Staging Project: proposals for the revision of the TNM stage groupings in the forthcoming (seventh) edition of the TNM Classification of malignant tumours. J Thorac Oncol 2007; 2: 706-714.
30. Schemper M, Smith TL. A note on quantifying follow-up in studies of failure time. Control Clin Trials 1996; 17: 343-346.
31. D'Agostino RB, Jr. Propensity score methods for bias reduction in the comparison of a treatment to a non-randomized control group. Stat Med 1998; 17: 2265-2281.
32. Rizvi H, Sanchez-Vega F, La K et al. Molecular Determinants of Response to Anti-Programmed Cell Death (PD)-1 and Anti-Programmed Death-Ligand 1 (PD-L1) Blockade in Patients With Non-Small-Cell Lung Cancer Profiled With Targeted Next-Generation Sequencing. J Clin Oncol 2018; 36: 633-641.
33. Kim Y, Hammerman PS, Kim J et al. Integrative and comparative genomic analysis of lung squamous cell carcinomas in East Asian patients. J Clin Oncol 2014; 32: 121-128.
34. Zheng CX, Gu ZH, Han B et al. Whole-exome sequencing to identify novel somatic mutations in squamous cell lung cancers. Int J Oncol 2013; 43: 755-764.
35. Brunelli M, Manfrin E, Martignoni G et al. Genotypic intratumoral heterogeneity in breast carcinoma with HER2/neu amplification: evaluation according to ASCO/CAP criteria. Am J Clin Pathol 2009; 131: 678-682.
36. Corbo V, Beghelli S, Bersani S et al. Pancreatic endocrine tumours: mutational and immunohistochemical survey of protein kinases reveals alterations in targetable kinases in cancer cell lines and rare primaries. Ann Oncol 2012; 23: 127-134.
37. Creighton CJ, Fu X, Hennessy BT et al. Proteomic and transcriptomic profiling reveals a link between the PI3K pathway and lower estrogen-receptor (ER) levels and activity in ER+ breast cancer. Breast Cancer Res 2010; 12: R40.

38. Landis JR, Koch GG. The measurement of observer agreement for categorical data. Biometrics 1977; 33: 159-174.

39. Bria E, Massari F, Maines F et al. Progression-free survival as primary endpoint in randomized clinical trials of targeted agents for advanced renal cell carcinoma. Correlation with overall survival, benchmarking and power analysis. Crit Rev Oncol Hematol 2015; 93: 50-59.

40. Bland JM, Altman DG. Measuring agreement in method comparison studies. Stat Methods Med Res 1999; 8: 135-160.

41. Conciatori F, Ciuffreda L, Bazzichetto C et al. mTOR Cross-Talk in Cancer and Potential for Combination Therapy. Cancers (Basel) 2018; 10.

42. Gkountakos A, Pilotto S, Mafficini A et al. Unmasking the impact of Rictor in cancer: novel insights of mTORC2 complex. Carcinogenesis 2018.

43. Janku F, Yap TA, Meric-Bernstam F. Targeting the PI3K pathway in cancer: are we making headway? Nat Rev Clin Oncol 2018; 15: 273-291.

44. Olaussen KA, Dunant A, Fouret P et al. DNA repair by ERCC1 in non-small-cell lung cancer and cisplatin-based adjuvant chemotherapy. N Engl J Med 2006; 355: 983-991.

45. Hammerman PS, Sos ML, Ramos AH et al. Mutations in the DDR2 kinase gene identify a novel therapeutic target in squamous cell lung cancer. Cancer Discov 2011; 1: 78-89.

46. Ricordel C, Lespagnol A, Llamas-Gutierrez F et al. Mutational Landscape of DDR2 Gene in Lung Squamous Cell Carcinoma Using Next-generation Sequencing. Clin Lung Cancer 2018; 19: 163-169 e164.

47. Wang JD, Jin K, Chen XY et al. Clinicopathological significance of SMAD4 loss in pancreatic ductal adenocarcinomas: a systematic review and meta-analysis. Oncotarget 2017; 8: 16704-16711.

48. Ziemke M, Patil T, Nolan K et al. Reduced Smad4 expression and DNA topoisomerase inhibitor chemosensitivity in non-small cell lung cancer. Lung Cancer 2017; 109: 28-35.

49. Devarakonda S, Rotolo F, Tsao MS et al. Tumor Mutation Burden as a Biomarker in Resected Non-Small-Cell Lung Cancer. J Clin Oncol 2018; JCO2018781963.

50. Owada-Ozaki Y, Muto S, Takagi H et al. Prognostic Impact of Tumor Mutation Burden in Patients With Completely Resected Non-Small Cell Lung Cancer: Brief Report. J Thorac Oncol 2018; 13: 1217-1221.